International Journal of Civil Engineering

Seismic Geotechnique

Liquefaction potential of reinforced silty sands

M. Alibolandi[1], R. Ziaie Moayed[2,*]

Received: July 2015, Revised: September 2015, Accepted: November 2015

Abstract

In this study a series of cyclic triaxial tests were performed to examine the undrained dynamic resistance of silty sand reinforced with various arrangements of geotextile layers. The silt content of samples varies in percentage from 0, 10, 20, 30, 40 and 50%. A total of 32 laboratory cyclic triaxial tests have been performed on silty sand samples reinforced with geotextile layers in different depths. All tests were performed with 100 kPa confining pressure, subjected to an isotropic consolidated undrained (CIU) condition. The tests were conducted at a frequency of 2 Hz. Results indicate that both the geotextile arrangement and the silt content were most essential in the liquefaction potential of reinforced sands. An increase in the number of geotextile layers enhanced the cyclic resistance of reinforced samples against the liquefaction potential. It was also found that when the geotextile layer was posited near the top of the specimen (load application part) the liquefaction resistance would increase (e.g. for clean sands, the improvement of liquefaction resistance caused by the geotextile layer had a 0.2 depth, and the sample height was 5.5 times greater than the geotextile layer inserted in mid height of sample H). Based on the obtained results, effects of geotextile on liquefaction resistance decreased as fines content increased to about 33%. Further increase in the fines content however, would lead to higher in reinforcement advantages. The liquefaction improvement is more effective with a higher number of geotextile layers. The results also revealed that the reinforcement effect in FC≈33 % is at its lowest amount.

Keywords: *Silt content, Liquefaction, Cyclic triaxial test, Geotextile arrangement.*

1. Introduction

Many types of geotextile reinforced soil structures are subjected to cyclic or dynamic loading. In some of these structures, cyclic loading conditions occur continual as transportation infrastructures, soil retaining walls and reinforced soil located beneath machine foundations. In the others, dynamic loading condition may only happen during earthquakes. Dynamic loading in undrained conditions can cause a destructive phenomenon called liquefaction.

According to the literature, soil liquefaction failures occur in saturated silty sands. Also, results reported by Ladd & Yamamuro [1] and Thevanayagam [2] indicate that sands deposited with silt content are much more liquefiable than clean sands. Moreover, deformation characteristics and pore pressure generation in silty samples are quite different from clean sand [3, 4].

Naeini and Baziar [5], indicate that the soil weakens as the silt content increases up to 35%, and then stronger than strengthens again; nonetheless, the clean sand remains the pure silt. Investigations of Polito and Martin [6] and Baziar and Sharafi [7] confirm the aforementioned results. Monkul and Yamamuro [8] found that if the mean grain diameter ratio ($D_{50\text{-sand}}/d_{50\text{-silt}}$) of the sand grains to silt grains is sufficiently small, the liquefaction potential of the sand increases steadily with increasing fines content for the studied range (0%–20%). As $D_{50\text{-sand}}/d_{50\text{-silt}}$ increases, the liquefaction potential of the silty sand might actually be less than the liquefaction potential of the clean sand. Sadrekarimi [9] indicates that the soil void ratio, the effective stress, and the shape and mineralogy of the fine particles can affect the liquefaction resistance of silty sands, allowing them to increase, decrease, or remain the same as the amount of fines content increases.

Effects of reinforcement on liquefaction susceptibility for clean sands have been previously studied [10,11]. Chandrasekaran et al. [10] identify shear stress mobilization as a function of normal stress and friction of soil-geotextile interface. Vercueil et al. [11] conducted various tests using a cyclic triaxial instrument, on samples of saturated Huston RF sand material. Reinforced with circular sheets of geo synthetic material, this sand has a uniform particle size range of D_{5o} = 0.38 mm and C_u =1.8 with e_{min} = 0.648, e_{max} = 1.041,. Tests performed with different types of geosynthetics, indicate a significant increase in liquefaction resistance for

** Corresponding author: Ziaie@eng.ikiu.ac.ir*

1 M. Sc.Graduated, Civil Engineering Department, Imam Khomeini International University, Qazvin, Iran

2 Associate Professor, Civil Engineering Department, Imam Khomeini International University, Qazvin, Iran

samples reinforced with compressible, non-woven geotextiles. According to test results obtained by Athanasopoulos et al. [12], the aperture ratio A/D_{50}, defined as the ratio of geotextile aperture size to the average sand particle size, affects the value of apparent interface friction angle, and attains its maximum value when $A/D_{50} \approx 1.60$.

Krishnaswamy and Isaac [13] denote that the increase in the liquefaction resistance of the reinforced soil is caused by increased effective confining pressure in the soil between the reinforcement layers, which is a function of the shear stress mobilized along the soil-reinforcement interface. They also founded that the reinforcement by higher stiffness increased the shear mobilization, while reinforcement by high compressibility reduced the shear mobilization.

Haeri et al. [14] carried out triaxial monotonic compression tests in order to determine the stress-strained dilation characteristics of geotextile-reinforced dry beach sand. The mechanical behavior demonstrated that geotextile inclusion increases the peak strength, the axial strain at failure, and the ductility of dry beach sand. However, it reduces dilation. Such improvements in the behavior of reinforced sand are more pronounced for small-sized samples. With an equal number of geotextile layers, geotextile arrangement is an essential parameter. Geotextile layers, properly placed either in the interception of the failure plane or in maximum tensile strain zones of unreinforced sand, are more effective than those randomly placed in other levels. An increase in the peak strength of geotextile-reinforced sand is influenced by the friction coefficient between geotextile and sand. By increasing this coefficient, the peak strength also increases.

Moghaddas Tafreshiand and Asakereh [15] conducted triaxial monotonic compression tests on wet (natural water content) non-plastic silty beach sand, both with and without geotextile reinforcement. The layer configurations that were used in the triaxial test samples included one, two, three and four horizontal reinforcing layers. Effects of the number of geotextile layers and confining pressures of 3%, 6%, 9%, 12% and 15% on strain levels were analyzed. They demonstrated that confining pressure causes a nonlinear increase in the strength of geotextile reinforced silty sands, a measure not effective under high confining pressures. Results also showed that an increase in the number of geotextile layer increases deviatoric stress (σ_d) to a specific value, leaving it at either constant or decreased value.

Liu et al. [16] carried out a series of undrained ring-shear tests were on saturated samples with different fiber content and sand density. Test results and mechanisms of fiber reinforcement indicate that the undrained shear behavior of fiber-reinforced loose samples is not greatly influenced by the presence of fiber, rather fiber presence affects the undrained behavior of medium dense and dense samples. Untreated specimens showed a continuous decrease in shear resistance after failure, while the specimens treated with fiber showed fluctuations even after shear failure. In fact, these fluctuations became even stronger with increasing fiber content. The peak shear strength also increases with the fiber content, especially in dense specimens. After shearing, all the fiber-reinforced and untreated dense samples maintained structural stability, while the unreinforced loose samples showed a complete collapse of structure.

Tuna and Alton [17] found that geotextile texture properties have important effects on interface shear strength and friction angle. For example, the non-woven geotextiles have a high horizontal deformation at failure and the least loss of strength after peak value. Undrained cyclic triaxial tests conducted by Ziaie Moayed and Alibolandi [18] investigate the shear modulus of saturated reinforced sand. The cyclic triaxial tests are conducted on remolded specimens, which were reinforced with different arrangement of non-woven geotextile. The G_{max} of saturated sand increased as the number of geotextile layer increased.

Naeini and Gholampoor [19] performed a series of cyclic triaxial tests to examine the behavior of dry silty sand samples reinforced with geotextile when subjected to dynamic loading. Results indicated that the geotextile inclusion and confining pressure increased the axial modulus and decreased the cyclic ductility of dry sand for all examined silt contents. In addition, it was found that by increasing the silt content up to about 35 percent the axial modulus in reinforced and unreinforced sand is decreased and cyclic ductility is increased. With further increases in silt content, these values are increased for cyclic axial modulus and decreased for cyclic ductility.

Noorzad and Amini [20] performed thirty stress-controlled cyclic triaxial tests on reinforced and non-reinforced saturated sands under undrained conditions. Test results indicated that the fiber inclusions significantly increased the liquefaction resistance of sand specimens. Increased fiber content and length led to more loading cycles of liquefaction. The reinforcement effect in medium dense samples was found to be more significant than that of looser samples.

Sayeed et al. [21] conducted a series of large-sized direct shear tests to determine the interfacial shear characteristics of sand–geotextile under three different normal stresses. Initial higher shear stiffness of sand-polypropylene geotextiles was observed corresponding to sand-hybrid geotextiles specifically under higher normal stresses.

In order to investigate the effects of principal stress rotation on the mechanical behavior of reinforced soil materials, Habibi et al. [22] carried out monotonic triaxial compression, triaxial extension and torsional shear tests on reinforced geotextile sand and clay. The tests were conducted on unreinforced and reinforced specimens with 2, 3 and 4 geotextile layers, and under three different confining pressures. Investigation of the monotonic behavior of the reinforced materials under different stress paths, i.e. triaxial compression, triaxial extension, and torsional shear shows that direction of principal stresses can have profound effects on the stress-strain curve, shear strength, and slope and intercept of the

failure envelope. Test results reveal that geotextiles improve the mechanical properties of both sand and clay. The strain at failure and undrained shear strength both showed increased geotextile layers in sand and clay. But even through geotextile inclusion enhanced the mechanical properties of geotextile reinforced sand and clay, it proved more effective in reinforcing sand.

Naeini and Eftekhari [23] performed a series of cyclic triaxial tests on sand with non-woven geotextile reinforcement to improve the liquefaction resistance. The layer configurations used include one and two horizontal reinforcing layers of a triaxial test sample. Influences of the number of geotextile layers, and cyclic stress ratio (CSR) were studied and described. Different CSR are selected to represent various loading induced in the soil by an earthquake. Results illustrated that the geotextile inclusion increases liquefaction resistance.

While considerable research has been conducted on the dynamic behavior of reinforced clean sands, not much information is available on the liquefaction resistance of geotextile reinforced silty sand. The aim of this research is to investigate the effects of geotextile reinforcement and its arrangement on the cyclic strength of silty sands. This study has undergone an elaborate program of cyclic triaxial tests at different cyclic stress ratios, different geotextile arrangements, and silt percentages (by weight) under undrained conditions.

2. Material Tested

The sand used in this study is Firouzkuh #161 crushed silica sand. Properties of this sand include its golden yellow color and uniform aggregation, giving it its name, Firouzkuh (Table 1). Firouzkuh sand has recently been used in laboratory stress-strain tests and studies on cyclic loading and liquefaction behavior. It has been identified as the standard sand in Iran (Ghahremani et al. [24], Baziar and Sharafi [7], Ghalandarzadeh and Ahmadi [25]). The silt used in this experiment was produced from grinding Firouzkuh sand and passing sieve no. 200. Table 2 presents properties of the non-woven PET geotextile used in this study.

Table 1 Firouzkuh #161 sand physical characteristics

Sand Type	G_s	e_{max}	e_{min}	D_{50} (mm)	C_u	C_c
Firouzkuh #161	2.68	0.943	0.603	0.28	1.87	0.88
Firouzkuh #161 + 10% silt	2.68	0.827	0.404	0.27	1.82	1.00
Firouzkuh #161 + 20% silt	2.68	0.860	0.359	0.26	22.3	8.59
Firouzkuh #161 + 30% silt	2.68	0.899	0.326	0.24	43.07	14.06
Firouzkuh #161 + 40% silt	2.68	1.0	0.336	0.23	60	16.13
Firouzkuh #161 + 50% silt	2.68	1.06	0.416	0.21	70.27	2.59

Table 2 Geotextile properties

Properties	Unit weight	Thickness	Puncture strength	Wide width tensile
ASTM method	D-5261	D-5199	D-4833	D-4595
Unit	gr/m^2	mm	N	kN/m
Value	500	3.5	1100	23.1

3. Test Procedure

The triaxial apparatus specimen included a 70 mm diameter with a height of 140 mm. A 70 mm diameter is ten times greater than the maximum particle size of used soil (d_{max} = 0.8 mm), which is recommended according to previous research (e.g., Wong et al. [26]). Further, membrane-compliance effects may be negligible for fine sands and silts tested in the conventional 71 mm diameter samples, since even very thin membranes cannot penetrate significantly into the small surficial voids (Nicholson et al [27]). The dry sand specimens were prepared according to the dry deposition technique of pouring sand through a funnel into a mold by maintaining a constant funnel zero height above the sand surface. The geotextile inclusions of 6.5 cm diameter are placed horizontally in the sample as each sand layer is formed. The specimens with different geotextile arrangements are shown in Fig. 2. It should be noted that the cyclic axial load was applied at the top of specimens, making the geotextile layer in B arrangement closer to the applying load than the layer in D arrangement. After the sample has been formed, the specimen cap is placed and sealed with O-rings, and a partial vacuum of 35 kPa is applied to the specimen to reduce the disturbances [28].

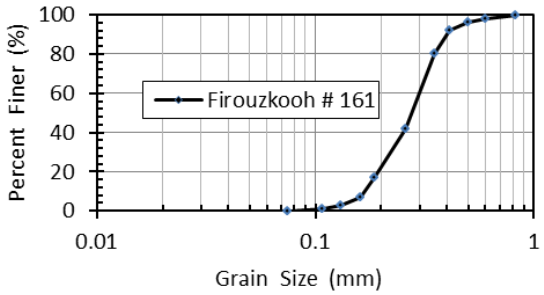

Fig. 1 Grain size distribution curve of Firouzkuh #16 sand

It should be noted that the main objective of the present research is to investigate the reinforcement effect on the liquefaction resistance in certain silt contents. In order to

fully saturate the specimen, CO_2-gas and de-aired water were used. After the water percolation period, the effective stress acting on the sample is kept constant by a parallel increase of cell and back pressures. The backpressure used varies from 10 to 90 kPa, which is sufficiently high to dissolve air bubbles and obtain Skempton B coefficients greater than 0.95. Following saturation, the specimens are consolidated isotropically at mean effective pressures of 100 kPa. Table 3 reports the specimens' void ratio at the end of consolidation (e_c). The void ratio of samples with the same silt content (and different geotextile arrangements) was nearly equal. For example, samples of clean sands and different geotextile arrangements (sample A – F) e_c were about 0.8.

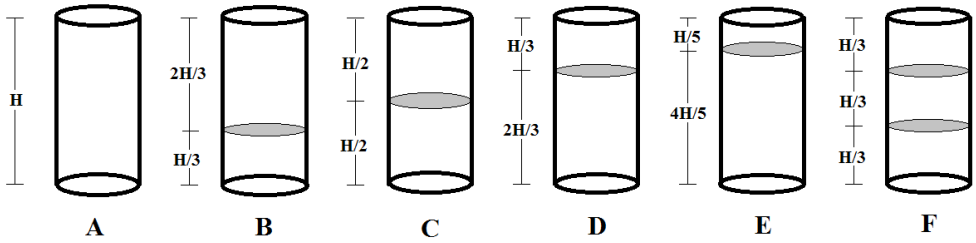

Fig. 2 Different geotextile arrangement in specimens

Table 3 Results of undrained cyclic triaxial tests

Test no.	FC (%)	CSR	Arrangement Type	Initial Elastic Modulus E(MPa)	Initial Shear Modulus G(MPa)	Liquefaction cycle for Ru=1	Liquefaction cycle for ε_{Da} =5%	e_c
1	0	0.3	A	6	2	4	15	0.80
2	0	0.3	B	9	3	4	11	0.80
3	0	0.3	C	11	4	5	21	0.80
4	0	0.3	D	16	5	12	40	0.79
5	0	0.3	D	16	5	8	11	0.80
7	0	0.3	E	18	6	15	41	0.79
6	0	0.3	F	18.75	6.25	15	50	0.80
8	0	0.25	F	13	4	20	70	0.80
9	0	0.35	F	9	3	8	34	0.79
10	0	0.45	F	7	2.5	6	7	0.79
11	10	0.275	A	11	4	5	11	0.70
12	10	0.275	C	27	9	5	13	0.70
13	10	0.275	F	23	8	22	22	0.70
14	10	0.15	F	1	0	Not liquefied	Not liquefied	0.70
15	10	0.3	F	7	2	5	11	0.70
16	20	0.15	A	5	1.6	48	77	0.57
17	20	0.15	C	25	8	62	73	0.57
18	20	0.15	D	24	8	63	70	0.57
19	20	0.15	E	31	10	65	72	0.57
20	20	0.15	F	49	16	Not liquefied	Not liquefied	0.57
21	25	0.15	F	17	6	360	441	0.57
22	30	0.15	A	18	6	98	19	0.57
23	30	0.15	C	23	8	Not liquefied	24	0.57
24	30	0.15	F	13	4	Not liquefied	42	0.57
25	40	0.15	A	2	1	Not liquefied	13	0.58
26	40	0.15	C	24	8	80	23	0.58
27	40	0.15	D	18	6	500	25	0.58
28	40	0.15	E	10	3	160	25	0.58
29	40	0.15	F	12	4	380	37	0.58
30	50	0.15	A	3	1	Not liquefied	20	0.58
31	50	0.15	C	19	6	Not liquefied	25	0.58
32	50	0.15	F	9	3	181	110	0.58

Based on ASTM D5311 [28], during undrained cyclic loading tests, the axial stress was cyclically measured in sinusoidal waves to load the samples at a frequency of 2 Hz. The cyclic liquefaction is considered to occur when one of the following conditions is satisfied:

1. Cancellation of effective stress ($R_u = u/\sigma_{cell} = 1$); [29]

2. Double amplitude axial deformation (ε_{Da}) greater than 5 %, [30].

Where u, σ_{cell} and R_u are pore pressure, confining pressure and pore pressure ratio, respectively.

Cyclic strength test results for isotropically consolidated specimens are often reported according to the number of cycles required for a specimen to reach various values of double amplitude axial strain or pore water pressure ratio, as opposed to the cyclic stress ratio (CSR):

$$CSR= \sigma_a/2\sigma'_{3c} \quad (1)$$

σ_a = average of peak cyclic stress in compression and extension, σ'_{3c} =effective isotropic consolidation stress

To enhance the assessment of reinforcement efficiency, the liquefaction improvement factor (*LIF)* is described as follows:

$$LIF = [(N_r-N_u)/ N_u] \times 100 \quad (2)$$

Where N_u and N_r are the numbers of liquefaction cycle for unreinforced and reinforced sample, respectively.

4. Results and Discussions

The liquefaction resistance of saturated sand mixed with varying amounts of non-plastic fines was evaluated by laboratory cyclic triaxial tests (Table 3). Test results were used to draw conclusions on the effect of fines content on the liquefaction potential of the reinforced and unreinforced samples. The conducted cyclic stress ratio of the test was selected to distinguish the liquefaction cycle of reinforced and unreinforced samples for certain silt content. Therefore, for sand with 10 % silt, CSR=0.275, and for other silt-sand mixtures CSR=0.15.

4.1. Effect of geotextile arrangement on liquefaction resistance

Fig. 3 compares results of the undrained cyclic triaxial tests by F type arrangement (Test No. 13), and unreinforced sample (Test No. 11) to the loading amplitude of 55 kPa (CSR=0.275). As shown in Figs. 3 (a) and 3 (b), axial strains are relatively small for the first 5 cycles of unreinforced samples, until substantial cyclically induced pore pressures have been generated. After about 5 cycles, the cyclic axial strain rapidly led to increased liquefaction triggering. As illustrated in Fig. 3 (c), the hysteresis loops show the shear stress versus the axial strain variations. Loop inclinations decrease as the number of loading cycles in the samples increase. This cyclic degradation occurs due to an increase in pore water pressure, causing the loops to flatten after the occurrence of liquefaction. Increasing rate in the pore pressure of reinforced samples remains low. After 22 cycles, there is a significant increase in the pore water pressure, along with significant developments in the double amplitude axial strain (5%), which lead to the liquefaction of the sample (Fig. 3 (c) and (d)). According to the obtained results, geotextile reinforcement considerably affects liquefaction of the samples. These figures indicate that reinforcement increases the liquefaction resistance of the samples considerably, in comparison to the unreinforced samples. This is mainly due to increased confinement. According to Yang's increased confinement concept, geotextile layers cause an internal confinement in reinforced samples [31].

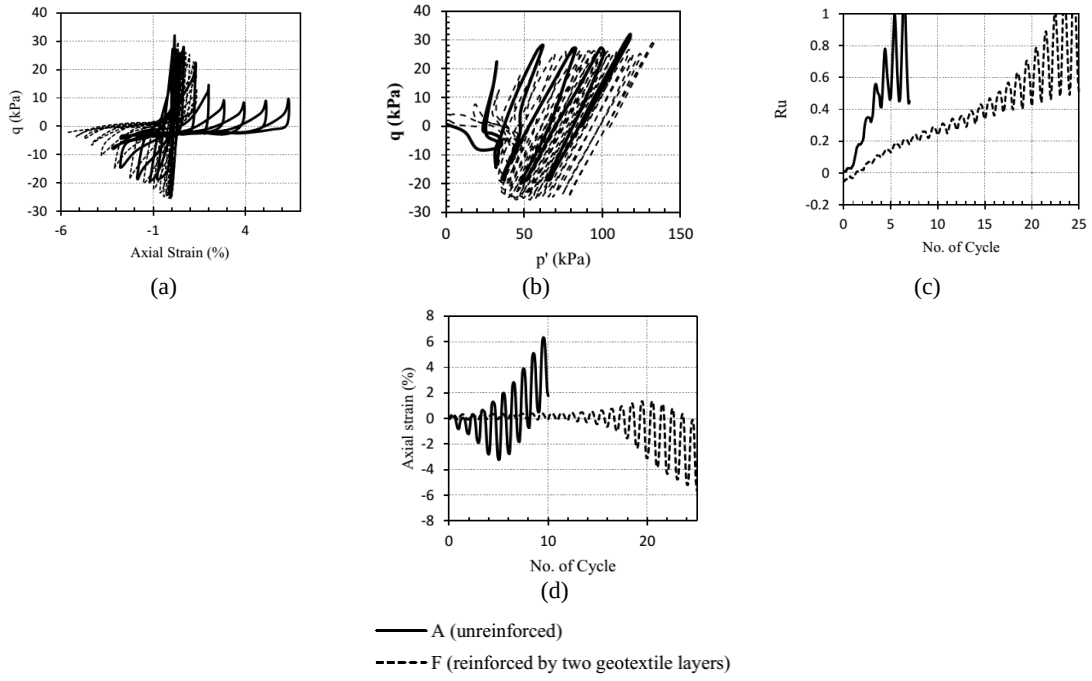

Fig. 3 Comparison of cyclic test results of unreinforced (A) and reinforced silty sand (10% silt) samples (F arrangement) CSR=0.275)

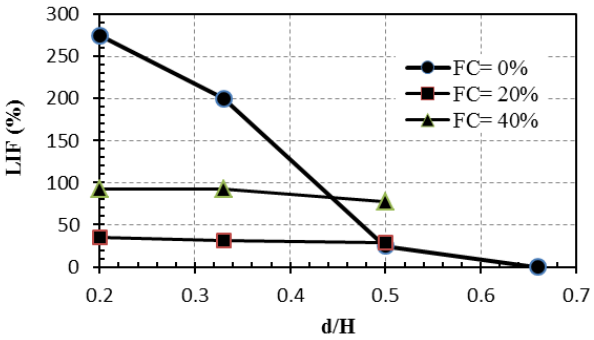

Fig. 4 Effect of depth of reinforcement layer (d/H) on LIF for reinforced sample by 1 layer geotextile

4.3. Effect of silt content on liquefaction resistance

Fig. 5 presents the liquefaction cycle for unreinforced samples with different silt content. Evidently, as the silt content increases to about 37%, the liquefaction cycle decreases. Further increase in silt content strengthens liquefaction, whereas a sample with 50% silt is weaker than the sand with 20% silt. This diagram is in accordance with the result of other investigations (e.g. [2], [6], and [8]). Thevanayagam [32] assumed that up to a certain fines content (Threshold Fine Content) the finer grains do not actively participate in the transfer of contact frictional forces, or their contribution is secondary. With this assumption, as a first-order approximation, all fines are assumed to be located within the voids in the coarser-grains matrix.

With significant increase in the fines content, the soil may be completely governed by the contacts along the fines, whereas the coarse grains will float within the fines. The presence of coarse grains has no effect on the force chain, except perhaps serving as a medium of contact between the many finer grains around it. Since it is not a void, nor does its volume affect the nature of the force chain in the finer grains, the volume of the coarse grains can be safely ignored.

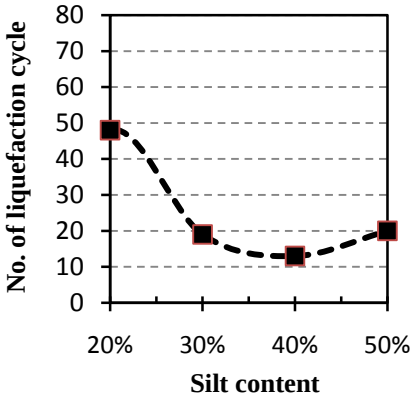

Fig. 5 Effect of silt content on liquefaction resistance of unreinforced silty sand samples (CSR=0.15)

Fig. 6 compares the liquefaction strength of reinforced and unreinforced samples versus silt content. The results indicate that a specimen reinforced with a 2-layer geotextile (F arrangement) is more efficient compared to a C-arrangement (1 layer of geotextile at mid height of sample). Fig. 6 illustrates the manner in which liquefaction resistance of reinforced samples decreases with the addition of non-plastic fines up to 33%. Beyond this critical value, the trend is reversed and the liquefaction resistance is increased with the increasing fines content. The effect of geotextile arrangement on the improvement of liquefaction resistance decreases as the samples' silt content increases. Increasing the silt content will reduce the internal friction angle and result in shear stress mobilization at geotextile-soil interface. This result is in accordance with research of Chandrasekaran et al. [10], which put forth that shear stress mobilization in the interface of geotextile and soil is a function of normal stress and friction at soil-geotextile interface.

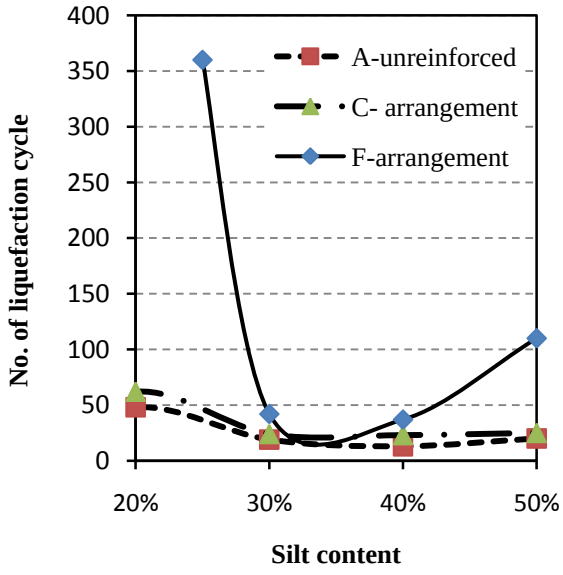

Fig. 6 Liquefaction cycle of reinforced and unreinforced samples versus silt content (CSR=0.15)

Illustrated in Fig. 7 is the Liquefaction Improvement Factor (LIF) of two-layered reinforcement samples (F arrangement) against the silt content. By increasing the mixture's silt content, the efficiency of geotextile reinforcement is reduced to the least amount possible of

FC=33%, and the efficiency is increased. This matter is justified due to the high liquefaction potential of the sample with 33% silt, which is liquefied before the mobilization of shear stress at soil-geotextile interface.

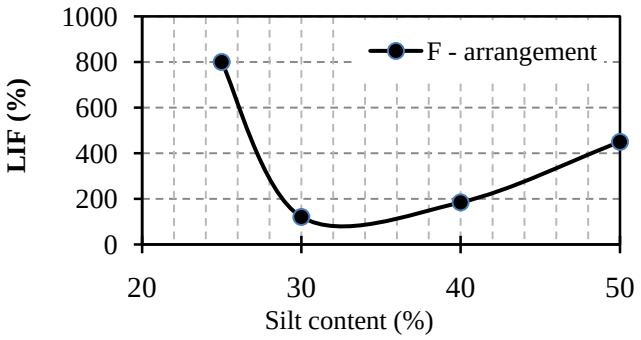

Fig. 7 Liquefaction Improvement Factor (LIF) of two layered reinforced samples vs. silt content. (CSR=0.15)

5. Conclusion

In the present study effects of silt content on geotextile-reinforced soil, and the cyclic strength of undrained silty sands was investigated. Results were verified using cyclic triaxial tests at different cyclic stress ratios, geotextile arrangements, and fines in undrained conditions. Based on the experimental results the following conclusions can be drawn:

- Geotextile inclusions increase liquefaction resistance, which depend on the arrangement and number of reinforced layers, as well as the amount of fines in the soil. As a result, geotextile layers cause increased internal confinement in the reinforced samples.
- The liquefaction improvement factor (LIF) of reinforced samples decreased as the ratio of geotextile layer depth to sample height (d/H) increased. In other words, liquefaction resistance is decreased as the depth of reinforcement is increased.
- Geotextile inclusion near the soil sample load is preferable. In depths greater than 0.66H, geotextile inclusion doesn't lead to increased liquefaction resistance. Geotextile field performance on liquefaction resistance of silty sand deposits depend on in-situ pore pressure dissipation conditions, namely depth and position of the drainage layer.
- The tensile force in the geotextile layer that develops as a result of the interfacial shearing resistance along the reinforcement length, significantly improves the sample's liquefaction resistance.
- For both reinforced and unreinforced samples, the liquefaction resistance initially decreases as the fines content increases up to 35 %. Further increase in the fine content however reverses the effect. Two-layered reinforced samples (F-Arrangement) showed higher significance than one-layered geotextile mid-height samples (C-arrangement). Efficiency of geotextile reinforcement decreases by increasing the fine content up to 33 %, which offer the least possible results. Due to the sample's high liquefaction potential with 33% silt, the sample liquefied before the shear stress was mobilized at soil-geotextile interface.
- Finally, it can be concluded that geotextile reinforcement increases liquefaction resistance of silty sand specimens. Inclusion of geotextile layers may therefore, be used to improve the liquefaction potential of silty sand deposits in engineering coastal purposes, including breakwaters, retaining wall soil backfilling, or strengthening of the road subgrade layer. Geotextile reinforcement are useful for any fine content; however; as the liquefaction potential of soils increase, efficiency of geotextile reinforcements decrease. Additionally, for efficient implementation of geotextiles, it is best to place them near the applying load, (e. g. upper side for traffic load and lower side for resisting against earthquake loads).

For purposes of furthering this research, the use of a large physical model such as a shaking table or a centrifuge model is recommended to identify the best location of geotextile layers.

Acknowledgements: The laboratory tests reported in this research were performed in the Geotechnical Laboratory at Imam Khomeini International University of Iran. This cooperation is thankfully appreciated. Furthermore, valuable comments of Dr. S.A. Naeini and Dr. M. Hassanlourad are gratefully acknowledged.

References

[1] Lade PV, Yamamuro JA. Effects of non-plastic fines on static liquefaction of sands, Canadian Geotechnical Journal, 1997, Vol. 34, pp. 918-928.
[2] Thevanayagam S. Effect of fines and confining stress on undrained shear strength of silty sands, Journal of Geotechnical and Geoenvironmental Engineering, ASCE, 1998, Vol. 124, pp. 479-491.
[3] Baziar MH, Dobry R. Residual strength and large-deformation potential of loose silty sands, JGT ASCE, 1995, Vol. 121, pp. 896-906.
[4] Baziar MH, Shahnazari H, Sharafi A. Laboratory study on the pore pressure generation model for Firouzkoohsilty sands using hollow torsional test, International Journal of Civil Engineering, 2011, No. 2, Vol. 9, pp. 126-134.
[5] Naeini SA, Baziar MH. Effect of fines content on steady-state strength of mixed and layered samples of a sand, Journal of Soil Dynamics and Earthquake Engineering, 2004, Vol. 24, pp. 181-187.
[6] Polito CP, Martin JR. Effects of nonplastic fines on the liquefaction resistance of sands, Journal of Geotechnical and Geoenvironmental Engineering, ASCE, 2001, Vol. 127, pp. 408-415.
[7] Baziar MH, Sharafi H. Assessment of silty sand liquefaction potential using hollow torsional tests - an energy approach, Soil Dynamics and Earthquake Engineering, 2011, Vol. 31, pp. 857-865.
[8] Monkul MM, Yamamuro JA. Influence of silt size and content on liquefaction behavior of sands, Canadian Geotechnical Journal, 2011, Vol. 48, pp. 931-942.
[9] Sadrekarimi A. Influence of fines content on liquefied strength of silty sands, Soil Dynamics and Earthquake Engineering, 2013, Vol. 55, pp. 108-119.

[10] Chandrasekaran B, Broms B, Wong KS. Strength of fabric reinforced sand under axisymmetric loading. Geotextiles and Geomembranes, 1989, Vol. 8, pp. 293-31.
[11] Vercueil D, Billet P, Cordary D. Study of the liquefaction resistance of a saturated sand reinforced with Geosynthetics, Soil Dynamics and Earthquake Engineering, 1997, Vol. 16, pp. 417-425.
[12] Athanasopoulos GA. Effect of particle size on the mechanical behavior of sand-geotextile composites, Geotextiles and Geomembranes, 1993, Vol. 12, pp. 255-273.
[13] Krishnaaswamy NR, Isaac NT. Liquefaction potential of reinforced sand, Geotextiles and Geomembranes, 1994, Vol. 13, pp. 23-41.
[14] Haeri SM, Noorzad R, Oskoorouchi AM. Effect of geotextile reinforcement on the mechanical behavior of sand, Geotextiles and Geomembranes, 2000, Vol. 18, pp. 385-402.
[15] Moghaddas Tafreshi SN, Asakereh A. Strength evaluation of wet reinforced silty sand by triaxial test, Iranian Journal of Civil Engineering, 2007, Vol. 4, pp. 274-283.
[16] Jin Liu, Gonghui Wang, Toshitaka Kamai, Fanyu Zhang, Jun Yang, Bin Shi. Static liquefaction behavior of saturated fiber-reinforced sand in undrained ring-shear tests, Geotextiles and Geomembranes, 2011, No. 5, Vol. 29, pp. 462-471.
[17] Tuna SC, Alton S. Mechanical behavior of sand-geotextile interface, Scientica Iranica, 2012, Vol. 19, pp. 1044-1051.
[18] Ziaie Moayed R, Alibolandi M. Influence of geotextile reinforcement on shear modulus of saturated sand, Proceedings of International Workshops on Civil Engineering, Koc University, Istanbul/Turkey, 2014, pp. 99-103.
[19] Naeini SA, Gholampoor N. Cyclic behavior of dry silty sand reinforced with a geotextile, Geotextiles and Geomembranes, 2014, Vol. 42, pp. 611-619.
[20] Noorzad R, Amini F. Liquefaction resistance of babolsar sand reinforced with randomly distributed fibers under cyclic loading, Soil Dynamics and Earthquake Engineering, 2014, , Vol. 66, pp. 281-29.
[21] Sayeed MA, JanakiRamaiah B, Rawal A. Interface shear characteristics of jute/polypropylene hybrid nonwoven geotextiles and sand using large size direct shear test, Geotextiles and Geomembranes, 2014, Vol. 42, pp. 63-68.
[22] Habibi MR, Shafiee A, Jafari MK. Monotonic behavior of geotextile reinforced soils under discrete rotation of principal stresses, IJST, Transactions of Civil Engineering, 2014, Vol. 38, pp. 325-335.
[23] Naeini SA, Eftekhari Z. Effect of geotextile on the liquefaction behavior ofsand in cyclic triaxial test, Proceedings of International Workshop on Civil Engineering and Architecture, IWCEA, 2014, Istanbul, Turkey, pp. 63-68.
[24] Ghahremani M, Ghalandarzadeh A, Moradi M. Effect of plastic fines on cyclic resistance of saturated sands (in Persian), Journal of Seismology and Earthquake Engineering, 2006, Vol. 8, pp. 71-80.
[25] Ghalandarzadeh A, Ahmadi A. Effects of anisotropic consolidation and stress reversal on the liquefaction resistance of sands and silty sands, Geotechnical Engineering Journal of the SEAGS & AGSSEA, 2012, Vol. 43, pp. 33-39.
[26] Wong RT, Seed HB, Chan CK. Cyclic loading liquefaction of gravelly soils, Journal of Geotechnical and Geo environmental Engineering, ASCE, 1975, Vol. 101, pp. 571-583.
[27] Nicholson RB Seed, Anwar HA. Elimination of membrane compliance in undrained triaxial testing, measurement and evaluation, Canadian Geotechnical Journal, 1993, No. 5, , Vol. 30, pp. 727-738.
[28] ASTM D5311-92. Standard Test Method for Load Controlled Cyclic Triaxial Strength of Soil, ASTM International, West Conshohocken, PA, 1992.
[29] Seed HB, Lee KL. Liquefaction of saturated sands during cyclic loading, Journal of the Soil Mechanics and Foundations Division, ASCE, 1966, SM6, Vol. 92, pp. 105-134.
[30] Dobry RS, Ladd FY, Yokel RM, Chung D, Powell, Prediction of pore water pressure build up and liquefaction of sands during earthquakes by the cyclic strain method. NBS Building Science Series 138, National Bureau of Standards, Gaithersburg, MD, 1982, 150.
[31] Yang Z. Strength and Deformation Characteristics of Reinforced Sand, Ph.D. Thesis, 1974.
[32] Thevanayagam S, Ravishankar K, Mohan S. Effects of fines on monotonic undrained shear strength of sandy soils, Geotech. Test GTJODJ, 1997, Vol. 20, pp. 394-406.
[33] ASTM D4833 (2013). An ASTM designation number identifies a unique version of an ASTM standard D4833 / D4833M - 07(2013)e1 D = miscellaneous materials; 4833 = assigned sequential number M = SI units 07 = year of original adoption (or, in the case of revision, the year of last revision) (2013) = year of last reapproval e1 = indicates editorial change Standard Test Method for Index Puncture Resistance of Geomembranes and Related Products.
[34] ASTM D4595 (2011). An ASTM designation number identifies a unique version of an ASTM standard. D4595 – 11 D = miscellaneous materials; 4595 = assigned sequential number 11 = year of original adoption (or, in the case of revision, the year of last revision) Standard Test Method for Tensile Properties of Geotextiles by the Wide-Width Strip Method.
[35] ASTM D5261 (2010). An ASTM designation number identifies a unique version of an ASTM standard. D5261 – 10 D = miscellaneous materials; 5261 = assigned sequential number 10 = year of original adoption (or, in the case of revision, the year of last revision) Standard Test Method for Measuring Mass per Unit Area of Geotextiles.
[36] ASTM D5199 (2012). An ASTM designation number identifies a unique version of an ASTM standard. D5199 – 12 D = miscellaneous materials; 5199 = assigned sequential number 12 = year of original adoption (or, in the case of revision, the year of last revision) Standard Test Method for Measuring the Nominal Thickness of Geosynthetics.